Local lattice expansion around Pd impurities in Cu and its influence on the Pd density of states: An extended x-ray-absorption fine-structure and Auger study

P. Weightman, H. Wright, and S. D. Waddington
Department of Physics, University of Liverpool, Oliver Lodge Laboratory, P.O. Box 147, Liverpool L69 3BX, United Kingdom

D. van der Marel and G. A. Sawatzky
Physical Chemistry Department of the Materials Science Center, University of Groningen, Nijenborgh 16, NL-9747 AG Groningen, The Netherlands

G. P. Diakun and D. Norman
Science and Engineering Research Council, Daresbury Laboratory, Warrington WA4 4AD, United Kingdom
(Received 10 April 1987)

The density of states of Pd in Cu given by impurity calculations is shown to be incompatible with the observed profile of Pd Auger transitions. Extended x-ray-absorption fine-structure experiments show that there is a local expansion of the lattice around Pd impurities in Cu but not in Ag. An analysis of the influence of the local lattice expansion on the electronic structure of *Cu*Pd alloys shows that it leads to a reduction in the intensity of the Pd density of states at the bottom of the band and yields a Pd density of states in good agreement with the observed Auger profile.

I. INTRODUCTION

The electronic structure of the Cu-Pd alloy system is currently the focus of a lot of experimental and theoretical work,[1–13] Recently Winter, Durham, Temmerman, and Stocks[5] have performed calculations of the electronic structure of Cu-Pd alloys in the self-consistent-field Korringa-Kohn-Rostoker coherent-potential-approximation (SCF-KKR-CPA) scheme. They argue that, contrary to earlier interpretations,[1–4] the electronic structure of Cu-Pd alloys dilute in Pd does not show the impurity virtual-bound state which is characteristic of similar systems such as *Cu*Ni and *Ag*Pd. Instead the Cu and Pd states share a common *d* band over the whole range of alloy compositions. However, the Pd density of states (DOS) given by the SCF-KKR-CPA calculations does not agree in detail with the results of a number of experimental probes of the Pd DOS.[9,11,12] This disagreement between SCF-KKR-CPA theory and experiment for the Cu-Pd system contrasts strongly with the situation for Ag-Pd alloys[14–21] where good agreement obtains between theory and experiment over the whole range of alloy compositions.

In this work we concentrate on a dilute alloy, $Cu_{95}Pd_5$, and evaluate the consistency between results for the Pd DOS and the experimental profile[7] of the Pd $M_{4,5}N_{4,5}N_{4,5}$ Auger spectrum. We show that the use of a Pd DOS given by a first-principles impurity calculation[13] leads to a disagreement between the calculated and experimental profiles of the Pd Auger spectrum similar to that obtained by using the Pd DOS given by the SCF-KKR-CPA calculations.[9]

We have measured the near-neighbor distances around Pd impurities, at the 1% level, in Cu by the extended x-ray-absorption fine-structure (EXAFS) technique and we find that there is a local expansion of the host lattice around Pd sites. We examine the possibility that the electronic structure of *Cu*Pd alloys is affected by this local expansion of the lattice and we have assessed its influence on the Pd DOS using a recent extension of the Clogston-Wolff model.[10] The extension to the model makes it possible to investigate the changes in the Pd DOS caused by variations in the nearest-neighbor host to impurity *d-d* hopping matrix element. By using Harrison's parametrization scheme[22] we are able to relate the local expansion of the lattice around Pd sites to the difference between the impurity-host and host-host *d-d* matrix elements. We find that allowing for the influence on the Pd DOS of the measured lattice expansion improves the agreement between the calculated and observed Pd Auger profiles.

Finally we show that the host lattice does not expand around Pd sites in *Ag*Pd alloys, suggesting that the agreement between experimental and theoretical results for the *Ag*Pd system and the disagreement for the *Cu*Pd system is due to the neglect of the local lattice expansion around Pd sites in the latter.

II. EXPERIMENT

Alloys of 1 at. % Pd in Cu and 1 at. % Pd in Ag were obtained from Metal Crystals, Ltd. (Cambridge, UK). The lattice constants of these materials and those of high-purity Ag and Cu were measured by x-ray diffraction using the Debye-Scherrer method. The results obtained for the nearest-neighbor distances from these measurements are shown in the first column of Table I. For Ag these results show that the addition of 1 at. % Pd causes a reduction in the average nearest-neighbor distances of $\simeq 0.0024 \pm 0.0004$ Å while the addition 1 at. % Pd to Cu results in an expansion of the average nearest-neighbor distance of $\simeq 0.0009 \pm 0.0005$

TABLE I. $Cu_{99}Pd_1$ and $Ag_{99}Pd_1$ near-neighbor distances, in angstroms.

	Average nearest-neighbor distance from x-ray diffraction	Near-neighbor distances from EXAFS					
		EXAFS analysis I			EXAFS analysis II		
		1st shell ±0.01	2nd shell ±0.04	3rd shell ±0.04	1st shell ±0.01	2nd shell ±0.04	3rd shell ±0.04
				$Cu_{99}Pd_1$			
Cu	2.5563(4)	2.515	3.54	4.39	2.564	3.60	4.46
Cu: $Cu_{99}Pd_1$	2.5572(3)	2.515	3.54	4.39	2.569	3.61	4.47
Pd: $Cu_{99}Pd_1$	2.5572(3)	2.560	3.55	4.41	2.614	3.60	4.50
				$Ag_{99}Pd_1$			
Ag	2.8889(3)	2.822	3.92	4.88	2.882	4.02	4.99
Ag: $Ag_{99}Pd_1$	2.8865(3)	2.827			2.889	4.04	5.02
Pd: $Ag_{99}Pd_1$	2.8865(3)	2.814	3.91	4.90	2.874	3.98	5.01

Å. However, it is possible that these small changes in average nearest-neighbor distances produced by the addition of Pd may mask larger changes in local near-neighbor distances around Pd sites. Consequently we determined the local near-neighbor distances directly by performing EXAFS experiments on these materials.

The EXAFS technique is ideal for determining near-neighbor distances.[23] Oscillatory structure in the photon absorption spectrum, caused by photoelectron scattering, has a frequency given by $\sin(2kR+\phi)$, where k is the photoelectron wave vector, R is the near-neighbor distance, and ϕ is the phase shift experienced by the photoelectron in the emission-backscattering process. These phase shifts are determined by the atomic cores and can be obtained by direct calculation. Since they are almost independent of the bonding configuration they can also be obtained empirically from elements or compounds with known geometry and then used to deduce distances in unknown specimens.

The EXAFS experiments were made on foils of between 20 and 30 micrometers in thickness obtained by rolling the materials. The EXAFS spectra were measured at the Daresbury Laboratory synchrotron radiation source using photons from the 5-T wiggler monochromated by a double-crystal (harmonic-rejecting) Si(220) arrangement.[24] Fluorescence detection, using scintillation counters,[25] was used to record the EXAFS spectra above the Pd K edge (24 350 eV) in the Ag_{99} Pd_1 and $Cu_{99}Pd_1$ alloys. Transmission spectra were measured for the Pd K edge absorption in pure Pd, the Ag K edge (25 514 eV) absorption in pure Ag and $Ag_{99}Pd_1$, and the Cu K-edge (8979 eV) absorption in pure Cu and the $Cu_{99}Pd_1$ alloy.

After subtracting the background the results of the EXAFS measurements were converted to k space and analyzed by a curve-fitting routine based on the rapid curved wave computational scheme[26] which included a least-squares iteration to give the best theoretical fit to the experimental data. Electron scattering phase shifts for Cu, Ag, and Pd as absorber and backscatterer atoms were calculated using a "muffin-tin"-potential–based method. The near-neighbor distances obtained from this analysis are shown in Table I (analysis I). The differences between the results for the nearest-neighbor distances in pure Cu and pure Ag obtained from x-ray diffraction and EXAFS is a well-known systematic effect caused by inaccuracies in the phase-shift calculations used in the EXAFS analysis. These systematic differences can be eliminated by modifying the Cu, Ag, and Pd phase shifts slightly so that the analysis of the EXAFS data obtained from the pure elements yields correct results for the near-neighbor distances. The well-established concept of phase-shift transferability[23] then allows the use of these corrected phase shifts for the determination of distances in the alloys. The near-neighbor distances obtained from this method of analyzing the EXAFS data are also shown in Table I (analysis II). Since in these experiments we are concerned with differences in distances between similar materials, most of the systematic errors in an EXAFS analysis cancel. The errors quoted in Table I arise almost entirely from small inaccuracies in transferring phase shifts between the analyses of data from the pure elements and the alloys and were estimated from the accuracy of the determination of known distances in the pure elements.

The analysis of the EXAFS data (Table I) shows that the small change in *average* nearest-neighbor distance (shown by x-ray diffraction) produced by the addition of Pd to Cu masks a larger *local* change around Pd sites. In $Cu_{99}Pd_1$ the EXAFS data yield an increase in the nearest-neighbor distance around a Pd site of 0.05±0.01 Å. This result is obtained from both methods of analyzing the EXAFS data, showing that, as expected, the systematic errors cancel. The EXAFS analysis also shows that the expansion is confined to the first shell of neighbors around a Pd site and that the near-neighbor separations around Cu sites are unchanged from those in pure Cu.

In $Ag_{99}Pd_1$ the EXAFS data are consistent with the view that there is no change in the host lattice around Pd sites, though it is possible that there is a slight contraction of the nearest-neighbor distance of ~0.01 Å, which is of the same order as the error limits of the EXAFS analysis.

III. THEORY: RELATIONSHIP OF AUGER PROFILE TO Pd DOS

We use, as our experimental probe of the Pd DOS of $Cu_{95}Pd_5$, the profile of the Pd $M_{4,5}N_{4,5}N_{4,5}$ Auger transitions as measured for this alloy composition by Weightman, Andrews, Stocks, and Winter.[7] In other alloy systems,[9,17,18,27–30] notably $Ag_{95}Pd_5$ (Ref. 17) and $Cd_{97}Ag_3$,[30] the Auger profile of the impurity has been shown to be a good test of models of the local impurity DOS. However, it is not a simple test since the Auger profile also depends on a number of other factors such as the correlation energy[31–35] of two hole states $U(L,S,J)$, which is dependent on the precise coupling of the L, S, and J quantum numbers of the two-hole final-state term structure, the transition rates to the various (L,S,J) terms,[36,37] the transition rate for the $M_4M_5N_{4,5}$ Coster-Kronig transition, and several mechanisms which broaden the observed Auger spectrum. Fortunately most of these effects are now understood for Pd impurity systems, as was demonstrated recently by the agreement obtained between theory and experiment for the Pd Auger spectrum of $Ag_{95}Pd_5$.[17] Provided the Pd Auger spectrum of $Cu_{95}Pd_5$ is interpreted carefully it can help to resolve the uncertainty in the Pd DOS in this alloy.

A. $M_{4,5}N_{4,5}N_{4,5}$ Auger groups and the $M_4M_5N_{4,5}$ Coster-Kronig transition

The Pd Auger spectrum consists of two groups of transitions, the $M_5N_{4,5}N_{4,5}$ group and, to higher kinetic energy, the $M_4N_{4,5}N_{4,5}$ group. The energy separation of the two groups is equal to the spin-orbit splitting of the initial state, 5.3 eV, which is accurately known from photoemission. The relative intensity of the two groups is strongly influenced by the transition rate for $M_4M_5N_{4,5}$ Coster-Kronig transitions which compete with $M_4N_{4,5}N_{4,5}$ transitions for M_4 initial-state holes and reduce the $I(M_5N_{4,5}N_{4,5}):I(M_4N_{4,5}N_{4,5})$ intensity ratio from 1.0:0.69, the value expected from calculations[38] of the initial-state photoelectron cross sections. The Coster-Kronig transition rate is very sensitive to the final-state conduction-band wave functions and might be expected to change with the Pd environment. In principle an upper limit on this transition rate can be established from the increased broadening of the M_4 relative to the M_5 photoelectron line, since the transition only contributes to the width of the former line. However, for Pd systems the Coster-Kronig broadening of the M_4 photoelectron line is small,[9,17,39] ~ 0.1 eV, and is difficult to determine even from high resolution, ~ 0.5 eV, photoelectron spectra. Consequently it is often necessary to treat the relative intensity of the Auger groups, $I(M_5N_{4,5}N_{4,5}):I(M_4N_{4,5}N_{4,5})$, as a variable parameter with a maximum value of 1.0:0.69. The analysis of the Pd Auger spectrum of $Ag_{80}Pd_{20}$ (Ref. 9) suggested a value of 1.0:0.3 for this ratio, corresponding to a lifetime broadening of the PD M_4 level of 0.1 eV. In the work reported here it was found that the optimum value for this ratio was 1.0:0.4 and that the effects on the calculated Auger profiles of varying this ratio were not strongly coupled to variations in other parameters.

B. Application of the Cini-Sawatzky model

For $Cu_{95}Pd_5$, measurements of the electronic specific-heat coefficient[40] and the observation of symmetric core level photoelectron lines[7] indicate that the density of states at the Fermi energy is low so that, within the context of the Cini-Sawatsky[31–33] treatment of conduction-band Auger processes, the Pd $4d$ band can be considered full. A further simplification of the situation is given by a consideration of crystal-field effects in analogous systems[41] which shows that it is reasonable to treat the (L,S,J) terms of the final-state multiplet structure independently.[28,42,43] With these provisos the Auger profile of each Auger group is given by

$$D(E)=\sum_{L,S,J}\frac{I(L,S,J)D^0(E)}{[1-U(L,S,J)H(E)]^2+\pi^2[U(L,S,J)]^2[D^0(E)]^2}\ , \tag{1}$$

where $D^0(E)$ is the self-convolution of $D^1(E)$, the conduction-band single-electron DOS. $H(E)$ is the Hilbert transform of $D^0(E)$, $U(L,S,J)$ is the Coulomb repulsion between two localized holes in the (L,S,J) term of the multiplet structure, and $I(L,S,J)$ is the Auger transition rate to the (L,S,J) component.

Equation (1) gives the calculated Auger profile as a function of the binding energy of the two-hole final states expressed relative to the Fermi energy. The experimental results are made consistent with this energy scale by subtracting the observed kinetic energy scale of the Auger spectrum from the binding energy of the core hole states measured by photoelectron spectroscopy.

C. The atomic multiplet structure

The position of the Pd final-state multiplet structure terms $U(L,S,J)$ are the same in each Auger group and are determined by the values of Coulomb Slater integrals $F^0(4d,4d)$, $F^2(4d,4d)$, $F^4(4d,4d)$, and the spin-orbit coupling ζ_{4d}. The magnitude of the spin-orbit coupling constant is largely determined by the atomic potential deep inside the atom and is not expected to change on the formation of the metal.[44–46] It should be given accurately by atomic structure calculations and we use $\zeta_{4d}=0.18$ eV, the value given by Hartree-Fock calculations using the Froese-Fischer code.[47]

It is well known that the value of the $F^0(4d,4d)$ Slater integral is greatly reduced from its value in the free atom by metallic screening. This produces a shift between the kinetic energies of Auger electrons observed from free atoms and metals. Since it affects the position of all the final-state (L,S,J) components equally we subsume it into the value of $U(^1G_4)$, the correlation energy for the most intense component, as a parameter to be used in calculating the Auger spectrum.

The $F^2(4d,4d)$ and $F^4(4d,4d)$ Slater integrals are largely responsible for the multiplet splitting of the (L,S,J) components. In metals with tightly bound d bands and large correlation energies, $U(L,S,J)$, the evidence suggests that the values of these Slater integrals are the same as they are in the corresponding free atoms. This can be seen from a comparison of the $M_{4,5}N_{4,5}N_{4,5}$ Auger spectra of atomic and metallic Cd (Ref. 48) which shows that the L-S-J splittings are the same in the two phases. This is also true of the elements following Cd.[49–51] Attempts to calculate the L-S-J splittings for these elements within the Hartree-Fock framework lead to overestimates, probably due to the neglect of relativistic and correlation effects.[46,49] Empirical reductions of the $F^2(4d,4d)$ and $F^4(4d,4d)$ integrals by $\sim$20% from the Hartree-Fock values give agreement with experiments.[46,49]

These observations on the elements Cd to Sn may not be a good guide for Pd systems since the Pd d band is less tightly bound and the $U(L,S,J)$ correlation energies are smaller. Furthermore the Pd Auger spectra of Pd alloys are strongly influenced by the band structure and it is difficult to determine the values of the Pd $4d^8$ Slater integrals from the shape of the Auger spectrum. Fortunately the Pd Auger spectrum of $Mg_{75}Pd_{25}$ is quasiatomic[29] and this spectrum has been used[17,52] to determine values of $F^2(4d,4d)$ and $F^4(4d,4d)$ for Pd of 6.02 and 3.94 eV, respectively. These values correspond to reductions of $\sim$34% from the results of Hartree-Fock calculations. The splittings of (L,S,J) components relative to the $^1G_4$ term calculated in intermediate coupling using these values of $F^2(4d,4d)$ and $F^4(4d,4d)$ and $\zeta_{4d}=0.18$ eV are shown in Table II.

Aksela, Harkoma, and Aksela[53] have recently published spectra of the $M_{4,5}N_{4,5}N_{4,5}$ Auger transitions of free Pd atoms. It is clear from these high-resolution spectra that the $4d^8$ final-state splittings of free Pd atoms are significantly larger than those shown in Table II. A careful study[52] of the effect on the calculated Pd Auger profile of changes in the Pd $4d^8$ splittings shows that the splittings are reduced in metals from the free-atom values and that the splittings of Table II are consistent with the observed profile of the Pd Auger spectra of $Mg_{75}Pd_{25}$,[17,52] $Al_{80}Pd_{20}$,[52] $Ag_{95}Pd_5$,[17,52] and $Ag_{80}Pd_{20}$.[9] We conclude that in Pd, but not in the elements Cd to Sn, metallic screening reduces the value of the $F^2(4d,4d)$ and $F^4(4d,4d)$ Slater integrals from their values in the free atom. Since the splittings of Table II agree with the Pd Auger profile observed from Pd alloys with Mg, Al, and Ag, we assume this effect is a consequence of the metallic state in general and that these splittings will also apply to $Cu_{95}Pd_5$, the alloy of interest here.

The relative intensities of the final-state multiplet structure components, $I(L,S,J)$, were calculated in the jj-intermediate coupling (jj-IC) scheme described by McGilp, Weightman, and McGuire[54] using McGuire's values of the radial integrals.[37] These results are shown in Table II. The results of our intensity calculations are in reasonably good agreement with the measurements of free-atom spectra,[53] particularly when it is remembered that several of the components are close together and it is experimentally difficult to separate their individual intensities. We would not expect exact agreement between our calculations and the free-atom results since in the jj-IC coupling scheme, appropriate to Pd, the $I(L,S,J)$ are influenced by the Slater integrals and since these are reduced in the metal by screening this will have a second-order effect on the $I(L,S,J)$ values.

We conclude that the multiplet structure of the Pd Auger transitions is well understood and that since the results of Table II give good agreement with the experimental Pd Auger profiles of $Mg_{75}Pd_{25}$,[17,25] $Al_{80}Pd_{20}$,[52] $Ag_{95}Pd_5$,[17,52] and $Ag_{80}Pd_{20}$,[9] they should also be appropriate to the Pd Auger profile of $Cu_{95}Pd_5$.

D. Broadening contributions

The observed Auger profile is affected by lifetime broadening and by contributions from the finite resolution of the instrument. The instrumental contribution to

TABLE II. Multiplet structure of the Pd $M_{4,5}N_{4,5}N_{4,5}$ Auger transitions.

(L,S,J) term[a]	Splittings (eV)	Relative intensities $M_4N_{4,5}N_{4,5}$	Relative intensities $M_5N_{4,5}N_{4,5}$
$^1S_0$	−2.41	2.28	2.55
$^1G_4$	0.0	27.69	24.48
$^1D_2$	0.22	21.38	5.92
$^3P_0$	0.30	5.43	3.20
$^3P_1$	0.32	8.89	5.91
$^3P_2$	0.73	7.57	14.47
$^3F_2$	1.33	9.45	9.13
$^3F_3$	1.49	14.89	10.06
$^3F_4$	1.89	2.42	24.28

[a]The L-S terms are mixed by spin-orbit coupling and are not pure states. The mixed states are denoted by the (L,S,J) component which makes the largest contribution to the corresponding eigenvector.

the Pd Auger profile of $Cu_{95}Pd_5$ can be represented as a Gaussian of full width at half maximum of (FWHM) 0.5 eV. The lifetime broadening can be represented as a Lorentzian of FWHM equal to the sum of the contributions from the lifetimes of the initial and final states. The contribution from the initial states is easier to establish since these states can be observed directly in the photoelectron spectrum. An analysis[52] of high-resoultion x-ray photoemission (XPS) measurements of the Pd M_5 core lines of $Mg_{75}Pd_{25}$ and $Ag_{95}Pd_5$ shows these to have lifetime broadening contributions of FWHM of 0.30 and 0.15 eV, respectively. These results are in reasonable agreement with the value of $\simeq 0.4$ eV found by McGuire[55] from atomic structure calculations. The additional lifetime broadening of the M_4 core hole state in $Ag_{95}Pd_5$ by the $M_4M_5N_{4,5}$ Coster-Kronig process, the rate for the latter having been determined from the relative intensity of the $M_4N_{4,5}N_{4,5}$ and $M_5N_{4,5}N_{4,5}$ contributions to the Pd Auger spectrum, is negligibly small ($\simeq 0.06$ eV).

The lifetime broadening of the two-hole final states is much harder to establish. For free Pd ions these states cannot decay by any intrinsic atomic process. In Pd metal and its alloys they can decay by dissociating into two independent hole states, the theory of which, with its influence on the Auger profile, is given by the Cini-Sawatzky model of the Auger process. Alternatively the two-hole states can decay by a further Auger process involving less-bound band states, V, which we can represent as $N_{4,5}N_{4,5}-N_{4,5}VV$. There has been no attempt to calculate the transition rates for such processes though the analogous case of the decay of a single deep hole state in a free-electron band was treated by Landsberg,[56] who concluded that the lifetime broadening at the bottom of the band was $\simeq 1.0$ eV. Fortunately it is possible to estimate the magnitude of such lifetime broadening processes by comparing the $M_{4,5}N_{4,5}N_{4,5}$ Auger profiles of free-atom and metallic Ag, Cd, In, and Sn. The best comparison is the work on free-atom and metallic Cd by Aksela, Aksela, Vuontisjarvi, Vayrynen, and Lahteenkorva,[48] who conclude that the metallic environment causes a lifetime broadening of these states by $\simeq 0.5 \pm 0.1$ eV. A similar result[50] holds for the elements In and Sn and after inclusion of the initial-state contribution this is consistent with the observation that the $M_{4,5}N_{4,5}N_{4,5}$ profiles of the elements Ag to Sn can be modeled by attributing a width of $\simeq 1.0$ eV to each (L,S,J) component.[46,49,50]

We conclude that in the free atoms the (L,S,J) components of the Auger transitions are narrow and their width is dominated by the lifetime broadening of the initial states. However, in the metals there is a significant contribution from the lifetime broadening of the final states, giving a total lifetime broadening of $\simeq 1.0$ eV to each (L,S,J) component. Thus as a working hypothesis we assume that in $Cu_{95}Pd_5$ the lifetime broadening contribution to the Pd Auger profile is $\simeq 1.0$ eV.

E. Background

The Auger and photoelectron spectra of solids are accompanied by a background of scattered electrons. The intensity of this contribution increases with decreasing kinetic energy so that the background count rate on the low kinetic energy of an Auger or photoelectron spectrum is higher than on the high kinetic energy side. It is often useful to add a simulation of this background contribution to a theoretical Auger profile so as to make a comparison with an experimental spectrum. In this work we assume that the background contribution to the spectrum at any energy is equal to a constant fraction of the total integrated intensity to higher kinetic energy. The magnitude of the constant is determined by the requirement of matching the background count rate to high energy and to low energy in the experimental spectrum. Although this procedure is a crude representation of the energy-loss processes, it does produce a smoothly varying background that agrees with experiment at the extremes of the experimental spectrum. Backgrounds of this form have been used in successful comparisons of theory with experiment for the $M_{4,5}N_{4,5}N_{4,5}$ Auger spectra of metallic Ag, Cd, In, and Sn (Ref. 49) of Ag alloyed with Mg,[28,52] Ag,[28,52] and Cd,[30] and of Pd alloyed with Mg,[17,52] and Ag.[9,17,52]

IV. DISCUSSION

The previous anlaysis shows that the Pd Auger profile is composed of two groups of transitions, $M_5N_{4,5}N_{4,5}$ and $M_4N_{4,5}N_{4,5}$, separated by 5.3 eV and with an intensity ratio which can take a maximum value of 1.0:0.69 but which is reduced to 1.0:0.4 by the effects of Coster-Kronig transitions. Each group is the envelope of a number of (L,S,J) components, the splittings and intensities of which are shown in Table II. The line shape of each component is specified by the Cini-Sawatzky model, (1), and is obtained from a self-convolution of $D^1(E)$, the local single electron DOS, by a distortion, the magnitude of which is given by the electron correlation energy $U(L,S,J)$. The profile will be broadened by a Gaussian instrumental contribution of 0.5 eV FWHM and by a Lorentzian lifetime broadening which we expect to be $\simeq 1.0$ eV. Finally the spectrum will be superimposed on a background of scattered electrons which we model as indicated in Sec. III E.

In order to use the Pd Auger profile as a test of results for the Pd DOS it is now only necessary to specify the correlation energy $U(^1G_4)$. However, since the kinetic energy spread of the Pd, $M_{4,5}N_{4,5}N_{4,5}$ Auger electrons is almost the same in all the Pd alloys studied so far it is likely that the value of $U(^1G_4)$ is almost independent of alloy composition. The results from studies on other systems lead us to expect that it lies in the range 2.8–3.1 eV: $U(^1G_4) \simeq 2.8$ eV for $Al_{80}Pd_{20}$,[52] 3.1 eV for $Mg_{75}Pd_{25}$,[17,52] and 2.8–3.1 eV for Ag-Pd alloys.[9,17,52] Restricting $U(^1G_4)$ to this range enables us to use the Pd Auger profile as a test of theoretical results for the Pd local DOS $D^1(E)$.

Braspenning, Zeller, Dederichs, and Lodder[13] have performed calculations of the electronic structure of impurities in Cu. Their results for the Pd DOS are shown in the inset to Fig. 1. The profiles of the Pd Auger transitions calculated according to the procedure out-

lined in Sec. III with $D^1(E)$ set equal to this DOS are shown in Fig. 1(a) for $U(^1G_4)=3.0$ eV and in Fig. 1(b) for $U(^1G_4)=2.5$ eV. In generating these Auger profiles the only free parameters are $U(^1G_4)$, the total intensity of the whole spectrum, and the $I(M_5N_{4,5}N_{4,5}):I(M_4M_{4,5}N_{4,5})$ intensity ratio which, as explained in Sec. III A has been fixed at 1.0:0.4. These profiles show that although the DOS from the impurity calculations can produce an Auger profile in rough agreement with the shape of that observed, it is displaced to high binding energy for values of $U(^1G_4)$ in the range expected. This overstimate of the binding energies of the two-hole DOS can be traced to the prediction of a high Pd DOS at the bottom of the band (Fig. 1). The calculated Auger profile can be shifted a little to lower binding energies by reducing the value of $U(^1G_4)$, as in Fig. 1(c) where $U(^1G_4)=2.0$ eV. However, this leads to a disagreement with the observed shape of the spectrum. We conclude that the results for the Pd DOS given by the impurity calculation are in poor agreement with experiment and that the agreement cannot be improved by varying $U(^1G_4)$ or by changing the procedure for calculating the Auger profile in any way which is consistent with the discussion of Sec. II.

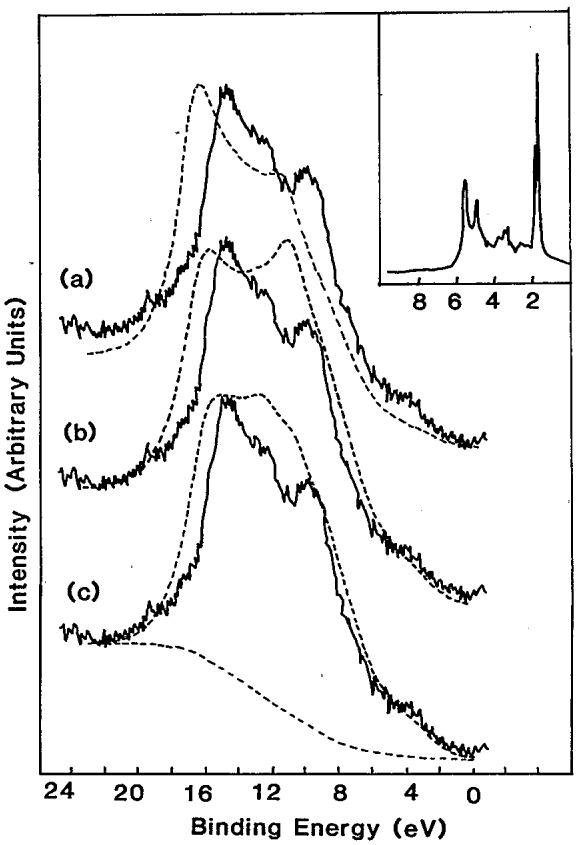

FIG. 1. The inset shows the Pd DOS of an isolated impurity in Cu given by the impurity calculations of Braspenning *et al.* (Ref. 13). In the main part of this figure and in the other figures the solid lines show the experimental profile of the Pd $M_{4,5}N_{4,5}N_{4,5}$ Auger transitions of *Cu*Pd measured by Weightman *et al.* (Ref. 7). The energy scale is appropriate to the $M_4N_{4,5}N_{4,5}$ Auger group and the zero of this scale is the Fermi energy. The energy scale for the $M_5N_{4,5}N_{4,5}$ Auger group is displaced by 5.3 eV to the left. The dashed lines show the Auger profiles calculated as described in the text. The calculated profiles shown here set $D^1(E)$ equal to the Pd DOS shown in the inset and $U(^1G_4)$ equal to (a) 3.0 eV, (b) 2.5 eV, and (c) 2.0 eV. The lower dashed line in (c) shows the background of scattered electrons calculated as described in Sec. III E.

An earlier study showed a similar disagreement between theory and experiment when $D^1(E)$ was taken from the results of SCF-KKR-CPA calculations.[5,9] In the earlier study[9] the agreement between theory and experiment was improved by arbitrarily reducing the Pd DOS, $D^1(E)$, at the bottom of the band, and recently[12] a direct determination of the Pd DOS in a concentrated Cu-Pd alloy has shown that SCF-KKR-CPA calculations[5] do overestimate the Pd intensity at the bottom of the band. It has been suggested[10,12] that a local expansion of the Cu lattice around a Pd site, an effect that is not allowed for in either the impurity[13] or the SCF-KKR-CPA[5] calculations, causes a reduction of the Pd DOS at the bottom of the band from the values that would occur in an undistorted lattice. The results of our analysis of the EXAFS data show that there is a local lattice expansion of about 2% around Pd sites in Cu. In order to estimate the effect of this expansion on the local DOS we need to relate the local nearest-neighbor distance to the electronic structure.

We adopt Harrison's scheme[22] relating the hopping matrix element between d states on atoms a and b, T_{dd}^{ab}, to the d-state radii r_d^a and r_d^b and the interatomic distance R^{ab}, by

$$T_{dd}^{ab} \propto \frac{(r_d^a r_d^b)^{3/2}}{(R^{ab})^5} . \tag{2}$$

We have $r_d^{\mathrm{Cu}}=0.57$ Å and $r_d^{\mathrm{Pd}}=0.94$ Å and for the elemental metals $R^{\mathrm{Cu\,Cu}}=2.55$ Å and $R^{\mathrm{Pd\,Pd}}=2.72$ Å. Using the results of the EXAFS analysis for $R^{\mathrm{Cu\,Pd}}$ gives $T_{dd}^{\mathrm{Cu\,Pd}}=1.4T_{dd}^{\mathrm{Cu\,Cu}}$. In the impurity calculation $R^{\mathrm{Cu\,Pd}}=R^{\mathrm{Cu\,Cu}}$, giving $T_{dd}^{\mathrm{Cu\,Pd}}=1.6T_{dd}^{\mathrm{Cu\,Cu}}$.

Having established how the local lattice expansion changes the hopping matrix element between the impurity and the host it is now necessary to determine how this affects the local Pd DOS. We use the modification to the Clogston-Wolff model of the local impurity DOS introduced by van der Marel, Jullianus, and Sawatsky.[10] The model Hamiltonian is written

$$H=\sum_k \varepsilon_k d_k^\dagger d_k+\sum n_k c_k^\dagger c_k+\Delta d_0^\dagger d_0+V\sum_k (c_k^\dagger d_0+d_0^\dagger c_k) + \sum_k \Delta T_k (d_k^\dagger d_0+d_0^\dagger d_k) , \tag{3}$$

where $d_k^\dagger$ and $c_k^\dagger$ refer to d-band and sp-band creation operators, respectively, the k subscript relating to the host and the 0 subscript to the impurity. The first four terms represent the standard Clogston-Wolff model. The d and sp bands of the host are represented by the first two terms, the interaction with the impurity state is described as a shift in the energy of the local d state by Δ

from the center $\langle \varepsilon_k \rangle$ of a host d band and a hybridization V between the impurity d state and the host sp band. The final term represents the extent to which the impurity-host d-d transfer integral $T_{\text{imp}}^{\text{host}}$ differs from the host-host d-d transfer integral $T_{\text{host}}^{\text{host}}$; in this case $\Delta T = T_{dd}^{\text{Cu Pd}} - T_{dd}^{\text{Cu Cu}}$. Van der Marel *et al.* show[10] that the addition of this extra term to the Hamiltonian leads to the local impurity DOS.

$$D^1(E) = \frac{1}{\pi} \operatorname{Im} \left[\frac{g_{d0}^{d0}}{(1+t)^2 - \{[(1+t)^2-1](E-E_d)+\Delta+V\} g_{d0}^{d0}} \right], \tag{4}$$

where E_d and g_{d0}^{d0} are, respectively, the centroid and the single-electron Green's function of the host d band and $t = \Delta T / T_{\text{host}}^{\text{host}}$. In this study we take the results for g_{d0}^{d0}, Δ, E_d, and V from previous work[10] which gave agreement with the photoelectron spectrum of *Cu*Pd.

Van der Marel *et al.*[10] show the changes in the impurity DOS predicted by (4) as a function of the value of t. For $t = -1$ the impurity is decoupled from the host and the model predicts an impurity DOS of a Lorentzian centered on $E_d + \Delta$. The standard Clogston-Wolff result is obtained with $t = 0$, corresponding to a local expansion of the lattice around the impurity so as to equalize $T_{\text{imp}}^{\text{host}}$ and $T_{\text{host}}^{\text{host}}$. As t is increased, more of the impurity DOS is mixed into the host d band and for $t = 0.6$ the model predicts an admixture comparable to that given by the impurity calculations.[13]

A. Comparison of model Pd DOS with Pd Auger profile

We now compare the Pd DOS predicted by the extended Clogston-Wolff model with the Pd Auger profile. The inset to Fig. 2 shows the Pd DOS predicted by the model when $t = 0.6$. As expected, this gives a strong contribution at the bottom of the band similar in intensity to that given by the impurity calculations but, of course, different in detail. The main part of Fig. 2 shows the Pd Auger profile derived from this DOS with $U(^1G_4) = 3.0$ eV. This calculation of the Auger profile shows a similar disagreement with experiment to that given by the impurity DOS (Fig. 1), and, as was found for the impurity case, reducing the value of $U(^1G_4)$ does not improve the agreement with experiment.

We now consider the effect on the Auger profile of using a Pd DOS generated from the model with a lower value of t, corresponding to a local expansion of the host lattice. Figure 3 shows the Pd DOS generated with t set at 0.4, the value appropriate to the lattice expansion found from the analysis of the EXAFS data, and the Auger profile generated from this DOS with $U(^1G_4) = 3.0$ eV. The Auger profile of Fig. 3 is in better agreement with experiment than those derived previously and this improvement in shape and position results from the reduction in the Pd DOS at the bottom of the band caused by the local expansion of the lattice. Al-

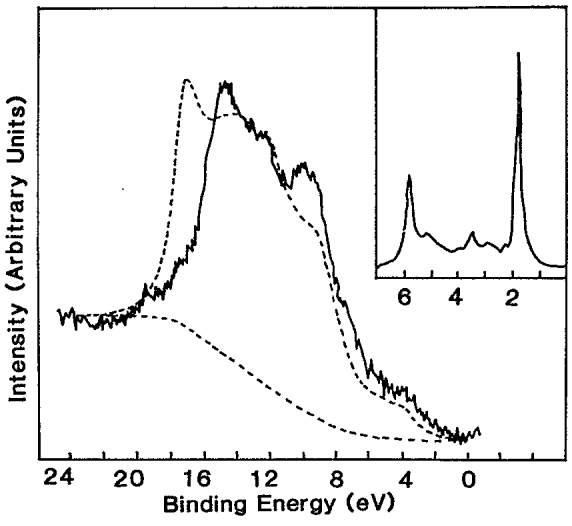

FIG. 2. The inset shows the Pd DOS given by Eq. (4) with $t = 0.6$. In the extension to the Clogston-Wolff model (Ref. 10) this value of t is appropriate to the unrelaxed lattice assumed in the impurity calculations (Ref. 13). The Auger profile calculated using this Pd DOS and $U(^1G_4)$ equal to 3.0 eV is shown by the dashed line.

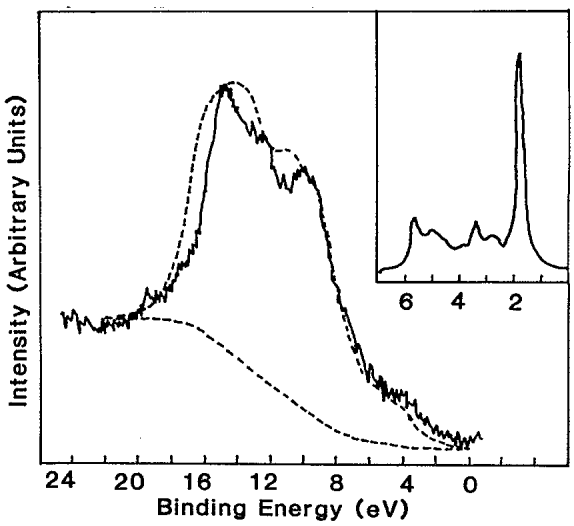

FIG. 3. The inset shows the Pd DOS given by Eq. (4) with $t = 0.4$. This value of t corresponds to the size of the expansion of the host lattice around a Pd site deduced from the analysis of the results of the EXAFS experiments. The Auger profile calculated using this Pd DOS and $U(^1G_4)$ equal to 3.0 eV is shown by the dashed line.

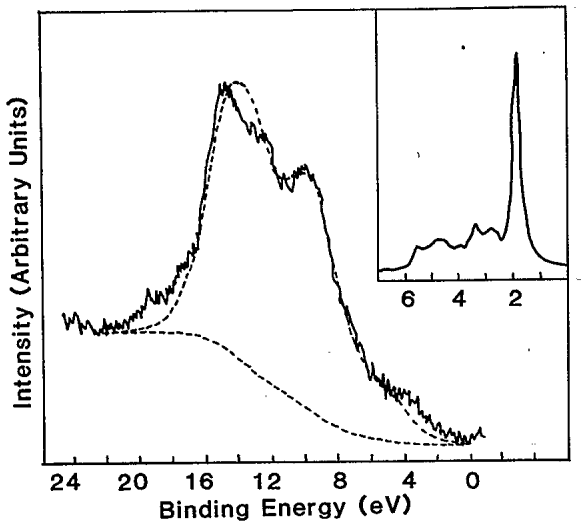

FIG. 4. The inset shows the Pd DOS given by Eq. (4) with $t=0.2$. This DOS gives the best agreement between theory and experiment when the Auger profile is calculated with $U(^1G_4)$ equal to 3.0 eV, as shown by the dashed line.

though the calculated Auger spectrum is not in perfect agreement with experiment it is in remarkably good agreement when it is remembered that all the ingredients used in generating the profile are either measured or chosen to be consistent with other experimentally determined quantities.

The main defect of the theoretical Auger profile shown in Fig. 3 is that it is broader than experiment. The width of the calculated profile is directly related to the intensity of the Pd DOS at the bottom of the band, which in the model is determined by the value of t. Reducing t to 0.2 leads to a further reduction in the Pd DOS at the bottom of the band and gives much better agreement with experiment, as shown in Fig. 4. Indeed the agreement between theory and experiment shown in Fig. 4 is as good as that obtained in the analysis of the Pd Auger profile in other alloy systems.

V. CONCLUSION

The analysis of the results of the EXAFS experiments show that there is a local expansion of the lattice around Pd sites in *Cu*Pd alloys but not in *Ag*Pd alloys. The calculations of the Auger profile show that, as expected from experience with other alloy systems, the Auger profile is very sensitive to the intensity of the component DOS at the bottom of the band and for *Cu*Pd the impurity calculations overestimate the intensity of the Pd DOS at the bottom of the band.

The changes in the Pd DOS which we expect to occur as a result of the local lattice expansion measured by EXAFS yield improvements in the calculated Auger profile. In terms of the extended Clogston-Wolff model, setting the parameter t at a value of 0.2 yields a Pd DOS consistent with the observed Auger profile.

These studies confirm that the previous disagreement between experimental and theoretical results for the *Cu*Pd alloy system is due to an overestimate by the theoretical calculations of the Pd DOS at the bottom of the band. A large part of this overestimate is due to the neglect of the local lattice expansion around the Pd site. The analysis of the results of the EXAFS experiments shows that there is no local lattice expansion around Pd sites in *Ag*Pd alloys.

ACKNOWLEDGMENTS

We are grateful to J. Baines of SERC Daresbury Laboratory for assistance in setting up the fluorescence EXAFS detectors. This work was supported by a Twinning Contract between the University of Liverpool and University of Groningen funded by the Committee for the European Development of Science and Technology (CODEST) of the Commission of the European Economic Community.

[1]J. Hedman, M. Klasson, R. Nilsson, C. Nordling, M. F. Sorokina, O. I. Kljuslinikov, S. A. Nemnonov, V. A. Trapeznikov, and V. G. Zynjanov, Phys. Scr. **4**, 195 (1971).
[2]S. Hufner, G. K. Wertheim, and J. H. Wernick, Solid State Commun. **17**, 1585 (1975).
[3]V. V. Nemoshkalenko, V. G. Aleshin, V. M. Pessa, and M. G. Chudinov, Phys. Scr. **11**, 387 (1975).
[4]N. Martensson, R. Nyholm, H. Calen, J. Hedman, and B. Johansson, Phys. Rev. B **24**, 1725 (1981).
[5]H. Winter, P. J. Durham, W. M. Temmerman, and G.M. Stocks, Phys. Rev. B **33**, 2370 (1986).
[6]R. S. Rao, A. Bansil, H. Asonen, and M. Pessa, Phys. Rev. B **29**, 1713 (1984).
[7]P. Weightman, P. T. Andrews, G. M. Stocks, and H. Winter, J. Phys. C **16**, L81 (1983).
[8]P. Weightman, M. Davies, and P. T. Andrews, Phys. Rev. B **30**, 5586 (1984).
[9]M. Davies and P. Weightman, J. Phys. C **17**, L1015 (1984).
[10]D. van der Marel, J. A. Jullianus, and G. A. Sawatzky, Phys. Rev. B **32**, 6331 (1985).
[11]S. C. Miller and P. T. Andrews, in Proceedings of the Institute of Physics Solid State Physics Conference, Southampton, U.K. 1984 (unpublished).
[12]H. Wright, P. Weightman, P. T. Andrews, W. Folkerts, C. F. J. Flipse, G. A. Sawatzky, D. Norman, and H. Padmore, Phys. Rev. B **35**, 519 (1987).
[13]P. J. Braspenning, R. Zeller, P. H. Dederichs, and A. Lodder, Phys. Rev. B **29**, 703 (1984).
[14]H. Winter and G. M. Stocks, Phys. Rev. B **27**, 882 (1983).
[15]H. Winter, P. J. Durham, and G. M. Stocks, J. Phys. F **14**, 1047 (1984).
[16]P. Weightman and P. T. Andrews, J. Phys. C **13**, L821 (1980).
[17]M. Vos, G. A. Sawatzky, M. Davies, P. Weightman, and P. T. Andrews, Solid State Commun. **52**, 159 (1984).
[18]P. Hedegard and B. Johansson, Phys. Rev. Lett. **52**, 2168 (1984).
[19]M. Vos, D. van der Marel, G. A. Sawatzky, M. Davies, P. Weightman, and P. T. Andrews, Phys. Rev. Lett. **54**, 1334 (1985).

[20]P. Hedegard and B. Johansson, Phys. Rev. Lett. **54**, 1335 (1985).
[21]P. Hedegard and B. Johansson, Phys. Rev. B **31**, 7749 (1985).
[22]W. A. Harrison, *Electronic Structure and the Properties of Solids* (Freeman, San Francisco, 1980).
[23]P. A. Lee, P. H. Citrin, P. Eisenberger, and B. M. Kincaid, Rev. Mod. Phys. **53**, 769 (1981).
[24]G. N. Greaves, G. P. Diakun, P. D. Quinn, M. Hart, and D. P. Siddons, Nucl. Instrum. Methods **208**, 335 (1983).
[25]J. T. M. Baines, C. D. Garner, S. S. Hasnain, and C. Morrell, Nucl. Instrum. Methods A **246**, 565 (1986).
[26]S. J. Gurman, N. Binsted, and I. Ross, J. Phys. C **17**, 143 (1984).
[27]P. Weightman, P. T. Andrews, and A. C. Parry-Jones, J. Phys. C **12**, 3635 (1979).
[28]P. Weightman and P. T. Andrews, J. Phys. C **13**, 3529 (1980).
[29]P. Weightman and P. T. Andrews, J. Phys. C **13**, L815 (1980).
[30]P. H. Hannah and P. Weightman, J. Phys. F **16**, 1015 (1986).
[31]G. A. Sawatzky, Phys. Rev. Lett. **39**, 504 (1977).
[32]M. Cini, Solid State Commun. **20**, 605 (1976).
[33]M. Cini, Solid State Commun. **24**, 681 (1977).
[34]G. A. Sawatzky and A. Lenselink, Phys. Rev. B **21**, 1790 (1980).
[35]V. Drchal and J. Kudrnovsky, Phys. Status Solidi B **108**, 683 (1981).
[36]E. J. McGuire, in *Atomic Inner-Shell Processes*, edited by B. Crasemann (Academic, New York, 1975).
[37]E. J. McGuire, Sandia Laboratory Report No. SC-RR-710075, 1971 (unpublished).
[38]J. H. Scofield, J. Electron Spectrosc. Relat. Phenom. **8**, 129 (1976).
[39]N. Martensson and R. Nyholm, Phys. Rev. B **24**, 7121 (1981).
[40]Y. Sato, J. M. Siversten and L. E. Toth, Phys. Rev. B **1**, 1402 (1970).
[41]M. Vos, D. v. d. Marel, and G. A. Sawatzky, Phys. Rev. B **29**, 3073 (1984).
[42]M. Cini, Phys. Rev. B **17**, 2788 (1978).
[43]A. Liebsch, Phys. Rev. B **23**, 5203 (1981).
[44]M. Blume and R. E. Watson, Proc. R. Soc. London, Ser. A **270**, 127 (1972).
[45]L. Ley, S. P. Kowalczyk, F. R. McFeely, and D. A. Shirley, Phys. Rev. B **10**, 4881 (1974).
[46]P. Weightman J. Phys. C **9**, 1117 (1976).
[47]C. Froese-Fischer, Comput. Phys. Commun. **4**, 107 (1972).
[48]S. Aksela, H. Aksela, M. Vuontisjarvi, J. Vayrynen, and E. Lahteenkorva, J. Electron Spectrosc. Relat. Phenom. **11**, 137 (1977).
[49]A. C. Parry-Jones, P. Weightman, and P. T. Andrews, J. Phys. C **12**, 1587 (1979).
[50]M. Pessa, A. Vuoristo, M. Vulli, S. Aksela, J. Vayrynen, T. Rantala, and H. Aksela, Phys. Rev. B **20**, 3115 (1979).
[51]S. Aksela, R. Kumpula, H. Aksela, J. Vayrynen, R. M. Nieminen, and M. Puska, Phys. Rev. B **23**, 4362 (1981).
[52]M. Davies Ph.D. thesis, University of Liverpool, 1985 (unpublished).
[53]S. Aksela, M. Harkoma, and H. Aksela, Phys. Rev. A **29**, 2915 (1984).
[54]J. F. McGilp, P. Weightman, and E. J. McGuire, Phys. C **10**, 3445 (1977).
[55]E. J. McGuire, Phys. Rev. A **5**, 1052 (1972).
[56]P. T. Landsberg, Proc. Phys. Soc. London, Sect. A **62**, 806 (1949).